Metabolic Engineering 91 (2025) 442–454

Contents lists available at ScienceDirect

Metabolic Engineering

journal homepage: www.elsevier.com/locate/meteng

A multilayered biocontainment system for laboratory and probiotic yeast

Carla Maneira [a,b], Sina Becker [b,1], Alexandre Chamas [b,c,d], Gerald Lackner [a,b,d,*]

[a] Faculty of Life Sciences: Food, Nutrition and Health, University of Bayreuth, Kulmbach, 95326, Germany
[b] Junior Research Group Synthetic Microbiology, Leibniz Institute for Natural Product Research and Infection Biology, Jena, 07745, Germany
[c] Department of Microbial Pathogenicity Mechanisms, Leibniz Institute for Natural Product Research and Infection Biology, Jena, 07745, Germany
[d] Cluster of Excellence Balance of the Microverse, Friedrich Schiller University, Jena, 07745, Germany

ARTICLE INFO

Keywords:
Biocontainment
Saccharomyces cerevisiae
Saccharomyces boulardii
Engineered live biotherapeutic products
Synthetic biology

ABSTRACT

The containment of genetically engineered microorganisms to designated environments of action is a paramount step in preventing their spread to nature. Physical barriers were traditionally employed to solve this issue, nevertheless, the growing number of biotechnological operations in open dynamic environments calls for intrinsic biocontainment. Here we describe the development of genetically embedded safeguard systems for both a laboratory strain of *Saccharomyces cerevisiae* and the commercial probiotic *Saccharomyces cerevisiae* var. *boulardii*. In a stepwise approach, single-input metabolic circuits based either on a synthetic auxotrophy or a CRISPR-based kill switch were developed before their combination into an orthogonal two-input system. All circuits are based on gut-active molecules or environmental cues, making them amenable to microbiome therapy applications. The final two-input system is stable for more than a hundred generations while achieving less than one escapee in 10^9 CFUs after incubation under restrictive conditions for at least six days. Biocontained strains can robustly produce heterologous proteins under permissive conditions, supporting their future use in the most varied applications, like *in-situ* production and delivery of pharmaceutically active metabolites.

1. Introduction

The advancements in metabolic engineering in the last decades account for the development of genetically modified microorganisms for a variety of industrial applications, such as the production of biofuels, chemicals, and pharmaceuticals (Katz et al., 2018; Clarke and Kitney, 2020; Maneira et al., 2025). Moreover, the recent engineering of probiotic microorganisms for direct therapeutic applications, known as engineered live biotherapeutic products (eLBPs), stands out as an alternative treatment for a series of ailments, enabling the on-demand production of bioactive compounds inside the human body (Chen et al., 2020a; Hedin et al., 2023a; Hwang et al., 2017; Isabella et al., 2018; Savage et al., 2023; Scott et al., 2021; Riglar et al., 2017; Tscherner et al., 2019; Rebeck et al., 2024). The economic and social potential of such technologies is massive, nevertheless, their propensity to cause environmental disbalances is a growing cause of concern. Genetically engineered microorganisms may bear hazardous genetic material, outcompete wild-type (Wt) populations, or even mutate into unsought phenotypes when released into the environment. Although the containment or selective removal of such microorganisms was historically carried out via physical barriers, the development of genomically embedded containment technologies stands out as a critical step in their transition from lab resources to real-life applications.

In light of this demand, the number of biocontainment strategies for engineered microorganisms has risen in the past years. Such systems typically rely on inputs specific to either permissive or restrictive settings to trigger survival-sustaining circuits or kill switches, respectively. Ultimately, they should allow for an escape rate of less than one escapee in 10^8 colony-forming units (CFUs) – as stated in the National Institute of Health (NIH) guidelines, address the possibility of horizontal gene transfer, and be stable in permissive conditions (Wilson, 1993). Many are the examples of biocontainment strategies with varying levels of success pertinent to engineered bacteria (Chan et al., 2016; Foo et al., 2024; Gallagher et al., 2015; Malyshev et al., 2014; Mandell et al., 2015; Rovner et al., 2015; Stirling et al., 2017; Rottinghaus et al., 2022). On the other hand, currently available biocontainment strategies for yeast, even if robust in specific contexts, are limited to particular frameworks and insufficient in the context of eLBPs (Hedin et al., 2023b; Hoffmann and Cai, 2024; Chang et al., 2023; Agmon et al., 2017; Cai et al., 2015; Yoo et al., 2020). Yeast biocontainment systems may be based on natural

* Corresponding author. Faculty of Life Sciences: Food Nutrition and Health, University of Bayreuth, Kulmbach, 95326, Germany.
E-mail address: gerald.lackner@uni-bayreuth.de (G. Lackner).
[1] Present address: Institute of Molecular Microbiology and Biotechnology, Faculty of Biology, University of Münster, Münster, 48149, Germany.

https://doi.org/10.1016/j.ymben.2025.06.009
Received 24 February 2025; Received in revised form 29 May 2025; Accepted 23 June 2025
Available online 25 June 2025

auxotrophies, i.e., dependency on natural growth factors such as amino acids (AAs) or vitamins (Hedin et al., 2023b). Although genetically stable, auxotrophies are susceptible to cross-feeding of growth factors under real-life conditions. On the other hand, approaches based on the transcriptional or translational control of essential genes by extrinsic factors (synthetic auxotrophies) are promising (Hoffmann and Cai, 2024; Chang et al., 2023; Agmon et al., 2017; Cai et al., 2015). Transcriptional control can be achieved by coupling the expression of essential genes with transcription factors responding to external stimuli. However, this strategy can encounter similar obstacles as natural auxotrophies, if the designed inputs are common to restrictive environments. For translational control of essential genes, the incorporation of unnatural AAs (unAAs) into essential genes via recoding of stop codons is a powerful strategy that was recently engineered in *S. cerevisiae* (Chang et al., 2023). Nevertheless, its portability to probiotic yeast species is still unknown, as well as the availability of unAAs in the gastrointestinal tract. Finally, systems that induce lethality via kill-switches were demonstrated to work well in artificial setups, nevertheless, in the framework of eLBPs, designs based on triggers that are either subjected to cross-feeding or lack universality of application are impractical (Agmon et al., 2017; Cai et al., 2015; Yoo et al., 2020). Circuits that trigger cell death via universal restrictive cues, such as temperature decay, circumvent these issues, however, no sufficient escape rate has been achieved until the moment (Hedin et al., 2023b).

In this work, we overcome these challenges, by engineering both a laboratory strain of *Saccharomyces cerevisiae* (Sc) and the commercial diploid probiotic *Saccharomyces cerevisiae* var. *boulardii* (Sb) with orthogonal intrinsic biocontainment modules that can be combined into a multiplex system for redundancy. First, we built artificial auxotrophies to anhydrotetracycline (aTc) by coupling the transcription of an essential gene to an improved version of the Tet-On system (Roney et al., 2016). This circuit allowed the engineered cells to survive only when aTc was provided. Next, we developed a kill switch, active solely at room temperature or lower, through the use of a temperature-activated version of the Gal4 protein (Gal4M9) (Zhou et al., 2018). This system elicited programmed cell death when coupled with CRISPR-Cas9 and a combination of single guide RNAs (sgRNAs) targeting different genomic regions. In a multiplex approach, we combined both the transcription switch and the best-performing kill switch, obtaining an orthogonal two-input system that restrains cell survival to aTc-rich environments at body temperature and leads to cell death when either room temperature is sensed or no aTc is provided. The final multiplex system was found to retain escape frequencies of less than 10^{-9} escapees/CFU for up to six days under restrictive conditions while remaining stable at permissive conditions for more than 100 generations. Furthermore, biocontained strains were able to produce heterologous proteins at levels comparable to the Wt, suggesting their amenability to different biotechnological applications.

2. Results and discussion

2.1. Preliminary chassis development

As a first step in the creation of biocontainment-enhanced strains, we designed natural auxotrophies to essential AAs. This allows the application of auxotrophy-based selection markers in plasmid systems (to avoid future work with antibiotic resistance cassettes) as well as the utilization of these *loci* as landing pads for future genomic modifications. The Sc strain (BY4741) used in this work is already auxotrophic to a variety of AAs (namely uracil, leucine, methionine, and histidine), nevertheless, genes *TRP1* and *LYS2* were knocked out to expand applications to tryptophan and lysine, respectively. For Sb, *loci TRP1*, *URA3* and *LYS2* were deleted (Fig. S1). However, as the knockout (KO) of *TRP1* was previously reported to cause growth defects in Sb in permissive conditions, strains with this genotype were abandoned (Hedin et al., 2023b). Natural auxotrophies can arguably be considered supplementary safety layers within genetically embedded biocontainment systems. However, given their potential for cross-feeding in natural environments, no AA-based auxotrophy was taken into consideration in characterization assays of the safeguard strains.

2.2. aTc-induced transcriptional switches

In order to establish a viable synthetic auxotrophy, the Tet-On system was chosen to drive the expression of an essential gene, ultimately coupling cell growth with the presence of inducers. Differently from other inducible systems based on molecules highly prone to cross-feeding (e.g. galactose or estradiol), critical concentrations of Tet-inducing molecules are unlikely to be found in natural environments unless provided (Dinh et al., 2017; Xu et al., 2015). On top of that, the system can be coupled with the tetracycline-derivative aTc, which works at lower concentrations and presents reduced antibiotic activity when compared to tetracycline (Gossen and Bujard, 1993; Chopra, 1994). aTc was previously found to be suitable for the engineering of gut commensals - it was delivered and bioactive in the gut of mice, where it effectively induced Tet-based circuits in engineered *E. coli* and *Bacteroides* sp (Rottinghaus et al., 2022; Lim et al., 2017). Nevertheless, Tet-On systems often display leaky background activity in yeast, which compromises their application. Agmon et al. tackled this issue by engineering the responsive promoter *pTET* to be compatible with safeguard circuits, however, activity under uninduced states persisted, jeopardizing the functionality of the system (Agmon et al., 2017). To overcome this problem, we employed the optimized Tet-On system described by Roney et al. as a transcriptional switch (Roney et al., 2016). The variant SE-G72P of the reverse tetracycline transcriptional activator (rtTA) – enclosing mutations V9I, F67S, F86Y, R171K, and G72P – and the responsive promoter *pTET4* – containing four rtTA binding sites – were selected because of their high sensitivity and tight regulation reported in Sc (Roney et al., 2016).

The system's performance in both strains was first evaluated in a dose-response curve with aTc as inducer and mRuby2 fluorescence as read-out (Fig. 1a-b). As expected, in Sc the transcription proved to be tight-regulated and fully activated in aTc concentrations as low as 1 μg/mL. The system was also shown to work in Sb strains with similar sensitivity. The minimal inducing concentrations were found to be under the toxicity limit for both yeast strains, in line with the findings reported by Baldera-Aguayo et al. (Fig. S2a) (Baldera-Aguayo et al., 2022). This concentration is also under the toxicity limit for human cells (Gossen and Bujard, 1993). Nevertheless, a considerable loss in the fluorescence intensity of the fully activated system was observed for Sb when compared to Sc. Given that the difference in fluorescence between the two strains is also observed with constitutively expressed mRuby2 (Fig. S2b–c), or when dox was used as the inducer of the Tet-ON system (Fig. S2d), we attribute this phenotype to particularities of Sb, such as its thicker cell wall, that might influence mRuby2 fluorescence (Hudson et al., 2016). To associate cell viability with aTc availability, the reporter gene was subsequently substituted for an essential gene (Fig. 1c). *RPC11*, coding for the subunit C11 of the RNA-polymerase II, was chosen due to its previous characterization as causing "very severe" phenotypes under a Tet-Off system, further confirmed under a galactose-inducible circuit (Cai et al., 2015; Mnaimneh et al., 2004). Expression of *RPC11* under threshold levels was demonstrated to cause lethality, while varied expression degrees above the silencing threshold maintained normal cell fitness, making it particularly amenable to inducible systems (Cai et al., 2015; Mnaimneh et al., 2004). Therefore, the promoter region of the *RPC11* gene was replaced by the responsive promoter for the optimized Tet-On system, *pTET4* (Fig. 1d). Final strains bearing the aTc-activated transcription switch were designated TS.

Fitness assessment of TS strains demonstrated normal growth patterns under the permissive condition (1 μg/mL aTc) and lethality under the restrictive condition (0 μg/mL aTc). The complete containment of engineered strains was achieved after approximately 16 h of exposure to

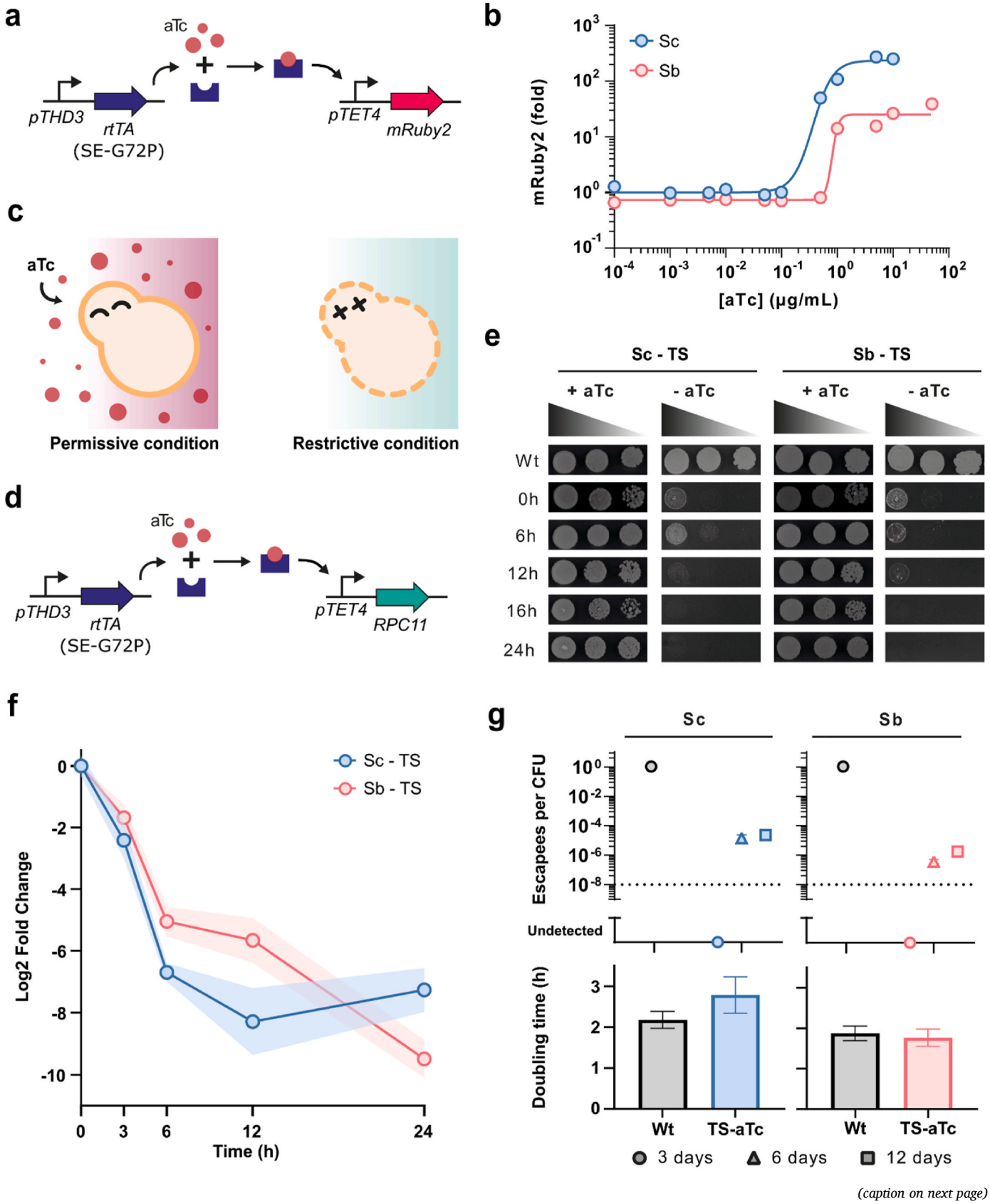

(caption on next page)

Fig. 1. The aTc-inducible transcription switch (TS)**. a** Schematics of the Tet-On system. In the presence of aTc, the expression of genes under the *pTET4* promoter is induced – in this case, *mRuby2*. **b** Sc and Sb strains carrying the *mRuby2* gene under the Tet-On system subjected to doses of aTc varying from 0.0001 to 100 μg/mL. Results are given in fold-change of mRuby2 fluorescence relative to the Wt. **c** A graphical scheme represents the functioning of the TS system. When submitted to permissive conditions (1 μg/mL aTc) cells survive. When transferred to restrictive conditions (no aTc) cells are no longer viable. **d** Schematics of the TS circuit. In the presence of aTc, the pTET4 promoter induces the *RPC11* essential gene. All parts are embedded in the genome. **e** Yeast dilution spot assay demonstrating the dependence of the TS strains on aTc. Cells were subjected to 0 to 24 h of restrictive treatment prior to plating. Plates were incubated for three days. **f** Time course of RPC11 gene expression in both Sc and Sb TS exposed to restrictive treatment (0 μg/mL aTc). Results are given in Log2 of the fold-change relative to basal expression levels at permissive conditions. **g Top** - Escape frequency of TS strains. Yeasts were subjected to 16 h of restrictive treatment prior to plating onto restrictive conditions. Plated cells were observed for up to twelve days for CFU formation. The assay limit was determined by the maximum CFUs plated, approximately 10^9. The black dotted line represents the NIH guideline for good containment. **Bottom** - Doubling times of TS strains cultivated under permissive conditions (1 μg/mL aTc) for 24 h. For all plots, values and error bars/envelopes are the average and standard deviation of biological triplicates, respectively.

the restrictive treatment, as observed in dilution spot assays performed at different time points (Fig. 1e). We, therefore, investigated *RPC11* expression levels in TS strains, switched from permissive to restrictive conditions, in order to determine whether the lengthy decay of the cells corresponded to the gene's transcription level. Samples for RT-qPCR were collected 0, 6, 12, and 24 h after the condition switch and normalized by the expression levels at time zero in order to obtain fold-change results (Fig. 1f). Approximately 6 h after exposing the strains to restrictive treatment, *RPC11* expression levels dropped by more than one order of magnitude, indicating that cells take circa 10 h longer than *RPC11*'s silencing patterns to die. This gap between the gene silencing and the phenotype visualization is likely due to the slow depletion of the remaining pool of C11 in the cell. Following this assumption, approximately five generations are necessary to eliminate the remaining C11 and consequently achieve containment after *RPC11*'s silencing. Substituting *RPC11* for an essential gene coding for a protein with a shorter half-life could mitigate this phenomenon, nevertheless, the number of efficient hits might be limited as the average protein half-life in Sc is 8.8 h (Christiano et al., 2014).

The aTc-activated biocontainment system achieved frequencies of escape mutants under one in 10^9 CFUs for both yeast strains when subjected to a 16-h restrictive treatment prior to plating (Fig. 1g, S3). Frequencies spanning 10^{-4} and 10^{-6} escapees/CFU were nevertheless observed for Sc and Sb, respectively, after twelve days of incubation, pointing towards the occurrence of late escape. The phenomenon of late escape is no stranger to yeast biocontainment systems. Indeed, previous safeguard strains based on different regulatory parts and inducers have also showcased escapees after six to ten days of incubation under restrictive conditions (Chang et al., 2023). Even though the underlying causes of late escape are unclear, we suspected late escapees to be mutants in which a severe growth impairment accompanies survival. To test this hypothesis, we monitored the growth patterns of late escapees in permissive and restrictive media (Fig. S4). Indeed, when compared to Wt cells, late escapees displayed a highly impaired growth profile under restrictive conditions (Fig. S4c–d). For Sc, a 2-fold greater doubling time was observed when compared to the Wt, while for Sb, a 5-fold increase in the doubling time was observed (Fig. S4e–f). Given that escapee frequency assessment was undertaken under ideal laboratory conditions and auxotrophies to amino acids were not taken into consideration, the effect of the growth defect on cell survival is anticipated to be even greater under natural conditions – where nutrient availability might be suboptimal and intra-niche competition can play a role.

As for the strains' performance in permissive conditions, TS strains showcased similar doubling time values to Wt strains, indicating system stability and low metabolic burden when aTc is provided (Fig. 1g).

2.3. CRISPR-based kill switches induced at room temperature

Alongside the development of transcriptional switches, whose activation sustains cell survival when aTc is provided, the construction of temperature-activated kill switches, whose activation is lethal at room temperature, was undertaken. The design holds the potential to halt fermentation via the containment of engineered yeast cells by refrigerating bioreactors, a feature potentially useful in both the food and pharmaceutical industries. In the context of eLBPs, it also takes advantage of the likelihood of contrast in temperature between the human body (37 °C – permissive condition) and the external environment (room temperature – restrictive condition). Recently, Hedin et al. have set the basis for temperature-activated safeguard systems in yeast (Hedin et al., 2023b). Through the KO of the *BTS1* gene, which codes for a geranylgeranyl diphosphate synthase, the authors achieved a strain that presents growth defects when exposed to temperatures of 15 °C or lower while maintaining normal growth under permissive conditions (Hedin et al., 2023b). Nevertheless, the development of a more sensitive system with less incidence of escape mutants remains pertinent (Fig. S5).

In order to activate the switch at room temperature or lower, the temperature-sensitive biosensor described by Zhou et al. was employed (Zhou et al., 2018). The approach is based on a mutant version of the Gal4 protein, Gal4M9, which is inactive at ≥30 °C and active at temperatures of 24 °C or lower. By knocking out the *GAL80* gene – to ensure Gal4 as the sole controller of the GAL regulatory network, and substituting *GAL4* for its mutant form, *pGAL* promoters are turned into temperature-sensitive transcription regulators (Zhou et al., 2018). The functionality of the temperature sensor was first evaluated in both Sc and Sb strains with fluorescence (*yeGFP*) as a readout (Fig. 2a-b). The system was overall tightly regulated under restrictive conditions (37 °C) for both strains. An increase in fluorescence of approximately two orders of magnitude was observed not only at the reported maximal inducing temperature of 24 °C but also at 26 °C. To comply with the standard definition of room temperature (IUPAC), 25 °C was used as inducing temperature in all subsequent assays.

Next, the temperature sensor was coupled with the CRISPR-Cas9 system to enable temperature-activated killing activity (Fig. 2c). For that, the *Cas9* gene was put under *pGal1* control, and constructs for the constitutive expression of sgRNAs were provided (Fig. 2d). The design takes advantage of the budding yeast's low viability when the repair of double-strand breaks (DSB) is undertaken via non-homologous end-joining (NHEJ) – i.e. when no repair template is provided (Dicarlo et al., 2013; Lemos et al., 2018). The *pGal1-Cas9* construct was first integrated into the *HO locus*, and different sgRNAs under the *pSNR52* snoRNA promoter were provided in *URA3*-based plasmids to evaluate their lethality. Three different genome-targeting sgRNAs, as well as combinations of them, were tested: a single-target sgRNA (*ADE2*), a sgRNA with multiple targets (*TY* retrotransposon delta sites), and a sgRNA with an essential gene as target (*SEC4*). Target *loci* were selected in order to investigate whether multiple DSBs could lead to greater lethality levels than a single DSB, or if disrupting a core gene could lead to less viability due to the greater impact of potential errors introduced by the NHEJ repair machinery. All sgRNAs applied to our circuit are highly efficient, with an average efficiency rate of more than 99 % (Fig. S6). They were also found to effectively disrupt both copies of DNA in the diploid Sb – a paramount step in the prevention of homology-based repair. Final strains bearing the temperature-activated CRISPR-Cas9 kill switch were nominated KS.

When tested under permissive and restrictive conditions in a dilution spot assay, all sgRNAs demonstrated killing activity under 25 °C (Fig. 2e). Except for the sgRNA targeting *ADE2,* that allowed colony formation when the highest cell density was applied, all other sgRNAs

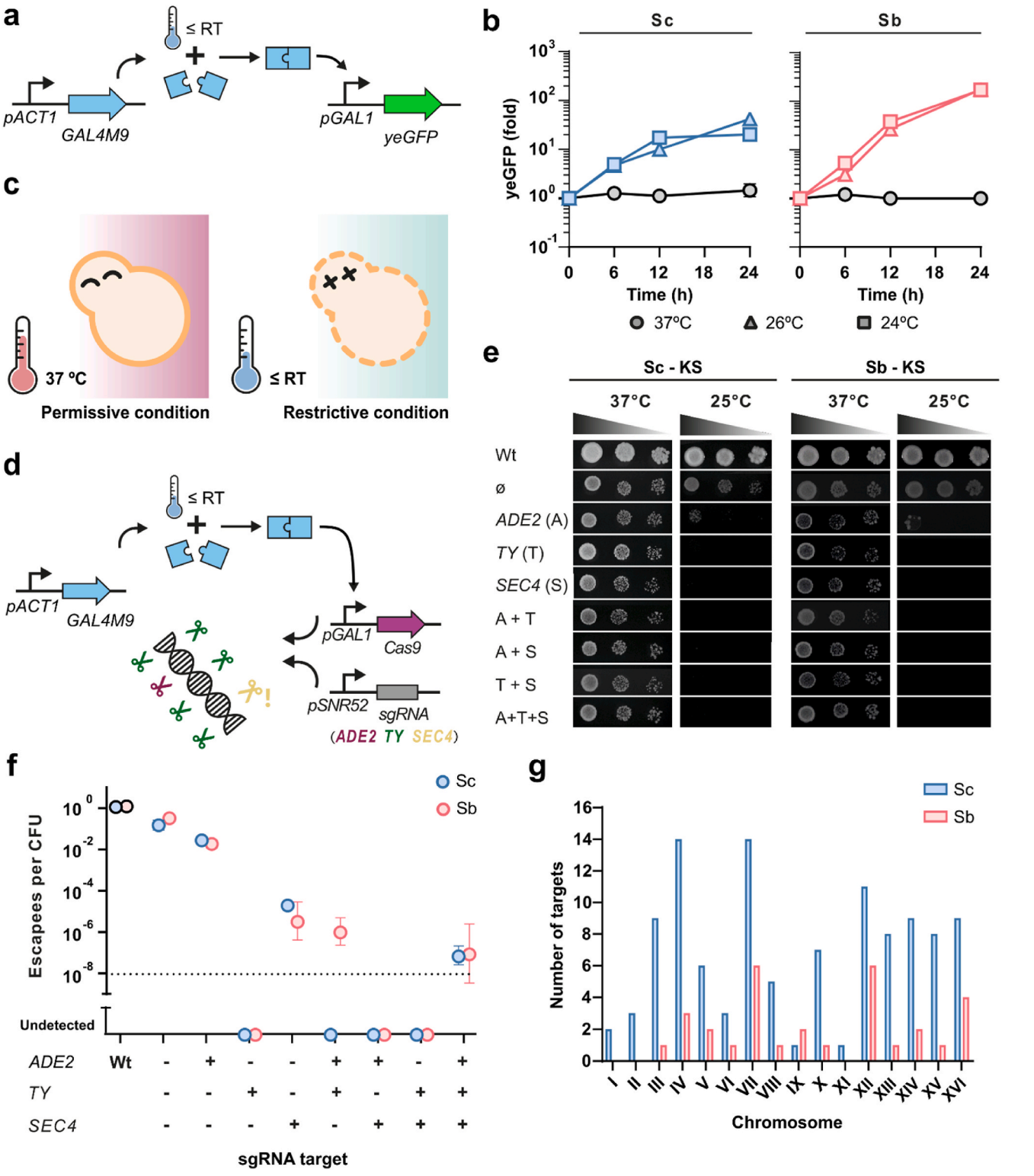

Fig. 2. The temperature-inducible CRISPR-Cas9-based kill switch (KS). **a** Schematics of the Gal4M9 temperature-sensitive system. Under RT or lower, the expression of genes under the *pGAL* promoters is induced - here *yeGFP*. **b** Characterization of the Gal4M9 temperature-sensitive system under permissive (37 °C) and restrictive temperatures (24 and 26 °C) in means of fold-change in yeGFP fluorescence for both Sc and Sb. **c** A graphical scheme represents the functioning of the KS system. When submitted to permissive conditions (37 °C) cells are able to survive. When transferred to restrictive conditions (25 °C or lower) cells are no longer viable. **d** Schematics of the KS system. Under RT, *pGAL1* drives Cas9 expression through the activity of Gal4M9. The Cas9 is then guided by one or many sgRNAs, leading to cell death by genome shredding. sgRNAs are provided in Ura-based plasmids. All other parts are embedded in the genome. **e** Yeast dilution spot assay demonstrating the dependence on temperature of the KS strains. Plates were incubated for three days. **f** Escape frequencies of KS strains. Colony formation was observed under restrictive condition for up to three days. The assay limit was determined by the maximum CFUs plated, approximately 10^9. The black dotted line represents the NIH guideline for good containment. **g** Number of functional (5′-sgRNA-NGG-3′) target sites for the *TY*-targeting sgRNA in all chromosomes of both Sc and Sb. A total of 110 and 31 (62 when considering Sb's 2n ploidy) target sites were found in Sc's and Sb's genomes, respectively. For all plots (except **g**), values and error bars represent the mean and standard deviation of biological triplicates, respectively.

and sgRNA combinations led to no viability under restrictive conditions. An escape frequency determination assay performed after three days of incubation gave more insight into the survival patterns (Fig. 2f, S7). Of the strains bearing a single sgRNA, only *TY*-targeting constructs lead to undetectable escapee numbers, supporting the hypothesis that a greater number of target *loci* significantly decreases the chances of survival. Even though Sb's genome contains approximately 39 % fewer target sequences for the *TY*-targeting sgRNA than Sc's (Fig. 2g), the effect was observed in both strains - indicating that the 62 targets in Sb's genome fall within the necessary threshold for effective killing under the assay limit of one in 10^9 CFUs. Interestingly, when reporting on a similar approach developed for bacteria-based systems, Rottinghaus et al. did not observe performance differences between single- and multiple-target sgRNAs (Rottinghaus et al., 2022). This disparity is most likely explained by the different repair systems used by each organism. While yeast relies on the NHEJ machinery to repair Cas9-induced DSBs when no repair fragment is provided, *E. coli* performs RecA-dependent homologous recombination using sister genomes as templates (Meddows et al., 2004).

As for sgRNA combinations, double-target constructs had overall excellent killing activity, with the exception of strain Sb KS-*TY* + *ADE2*, which exhibited escape frequencies of approximately 10^{-6} escapees/CFU. Also interesting were the results obtained for strains bearing all three sgRNAs. Instead of exhibiting an additive effect, both Sc and Sb displayed approximately 10^{-7} escapees/CFU, suggesting that single sgRNAs with high killing impact might be more efficient than a combination of sgRNAs with varying levels of killing activity. This phenomenon might be directly related to the overall lower efficiency of the CRIPSR-Cas9 system in multiplex settings in yeast (Ryan et al., 2014; Mans et al., 2015). In this scenario, the greater number of escapees in multi-sgRNA designs is most probably caused by a decrease in DSB performance - and consequently cell death - rather than the emergence of escape mutants. Also concerning the application of multiple sgRNAs, results in *E.coli* point in the other direction - in this organism, the combination of sgRNAs resulted in lower escape rates (Rottinghaus et al., 2022). Nevertheless, the discrepancy is due to a design difference. In the bacterial system published by Rottinghaus et al., not only the Cas9, but also all sgRNAs were under aTc-responsive promoters, meaning that the redundancy of regulating elements was increased with the number of sgRNAs (Rottinghaus et al., 2022).

In light of these findings, we have opted not to explore the triple-sgRNA design. The *ADE2*-targeting sgRNA was also discarded due to its low killing efficiency, likely caused by moderate NEHJ competency (Fig. S8). Further characterization and improvement rounds were therefore carried out for both Sb and Sc-based systems containing the two most promising constructs: KS-*TY* and KS-*TY* + *SEC4*.

2.4. Improved kill switch stability through the addition of a degron tag

Even though the KS strains achieved exceptional killing efficiency alongside a low number of escape mutants at room temperature, significant growth impairment was observed under permissive conditions in solid medium – KS strains grew slower when compared to the Wt (Fig. 2c). Severe growth deficiencies in permissive conditions exert strong selective pressure on engineered strains (Lee et al., 2018). Therefore, the pronounced fitness penalty is likely to increase the occurrence of escape mutants. We hypothesized that the leakiness of the temperature switch caused the phenotype. To solve the issue, we relied on the application of a degradation tag (degron) for the post-translational control of protein expression. Instead of coupling the degron to Gal4M9 - which is constitutively expressed but only active at room temperature or lower due to a conformational change - we opted to enhance Cas9 degradation. Through these means, we expected to reduce the detrimental impact of circuit leakiness under permissive condition, while maintaining functionality in the restrictive environment, where high expression levels are expected. Therefore, a shortened version of the C-degron of PEST-tag's MAX isoform E, isoE, described by Peter et al., was added to the C-terminus of the Cas9 (Peter et al., 2021). Strains bearing this design were named KS-IsoE (Fig. 3a).

Both KS and KS-IsoE strains bearing the most promising sgRNA combinations (TY and TY + SEC4), were evaluated in a similar fashion as performed for TS strains. When cultured for 24 h in permissive liquid medium, a reversion of the growth penalty was observed, with KS-IsoE strains showcasing ΔOD_{600} values comparable to the Wt while KS strains exhibited highly impaired growth (Fig. 3b). An equivalent result was obtained when cells were submitted to dilution spot assays in solid medium (Fig. 3c). KS-IsoE strains showcased similar spot formation patterns as the Wt under permissive conditions.

Under room temperature, on the other hand, cells submitted to dilution spotting either exhibited reduced colony formation or the complete absence of colonies, indicating the persistence of circuit functionality (Fig. 3c). When submitted to an escape frequency determination assay, all systems achieved frequencies of escape under one in 10^9 CFUs with the exception of strain Sc KS-IsoE-TY + SEC4, which showcased approximately 10^{-6} escapees/CFU already on day 3 of incubation (Fig. 3b, S9). Escape frequencies spanning 10^{-7} and 10^{-5} escapees/CFU were nevertheless observed after twelve days of incubation for all other KS-IsoE strains (Fig. 3b). In general, the addition of the degron tag led to the inflation of escape rates. Nevertheless – except for the aforementioned strain Sc KS-IsoE-TY + SEC4, which showcased a considerable difference in escape frequency when compared to its counterpart without degron – the effect was moderate and only observed in prolonged incubation (six and twelve days). This suggests that the presence of the degron indeed impacts the levels of Cas9 even under restrictive conditions, however, the effect is presumably dampened by the high expression levels of the protein. It is also worth noting that, just as in KS strains, the greater killing performance of a single efficient sgRNA over a combination of sgRNAs of varied efficiencies was observed for KS-IsoE. A pattern we attribute to the lower efficiency of CRISPR-Cas9 multiplex systems in yeast (Ryan et al., 2014; Mans et al., 2015).

When further analyzed for their performance under permissive conditions, all KS-IsoE strains showcased similar doubling times as the Wt (Fig. 3d). In light of the improvement of the degron tag over the KS performance in permissive medium and the low escape rates observed after twelve days of incubation, we decided to move forward with strains Sc and Sb KS-IsoE-TY.

2.5. A two-input biocontainment system responds to both aTc and room temperature

To develop a two-input biocontainment system that constrains cell viability to aTc-supplemented environments and induces lethality in response to a temperature downshift, both biocontainment systems were combined (Fig. 4a). Final strains bearing both the TS and the KS-IsoE + TY systems were designated TS-KS. When tested for their fitness, four different conditions were evaluated: one permissive (37 °C, 1 μg/mL aTc), two single-input restrictive (37 °C, no aTc and 25 °C, 1 μg/mL aTc), and one fully restrictive (25 °C, no aTc) – permitting the comparison of respectively none, single and both biocontainment system's activity. Whenever aTc-poor conditions were evaluated, cells were submitted to medium without aTc for 16 h prior to assessment, to comply with the slow phenotype switch of strains bearing the TS circuit.

Dilution spot assays performed under all conditions revealed expected phenotypes, with both TS-KS strains thriving under permissive conditions while not growing in all other conditions (Fig. 4b). When evaluated for their escape frequencies under semi-restrictive conditions, both Sb and Sc TS-KS led to numbers similar to the observed when only one of the biocontainment systems was employed, suggesting that the two-input system performance remains close to that of its single-input counterparts (Fig. 4c, S10). Under fully restrictive conditions, a substantial decrease in the escape rate was observed (Fig. 4c, S10). No escapees were found for Sb even after twelve days of incubation. For Sc,

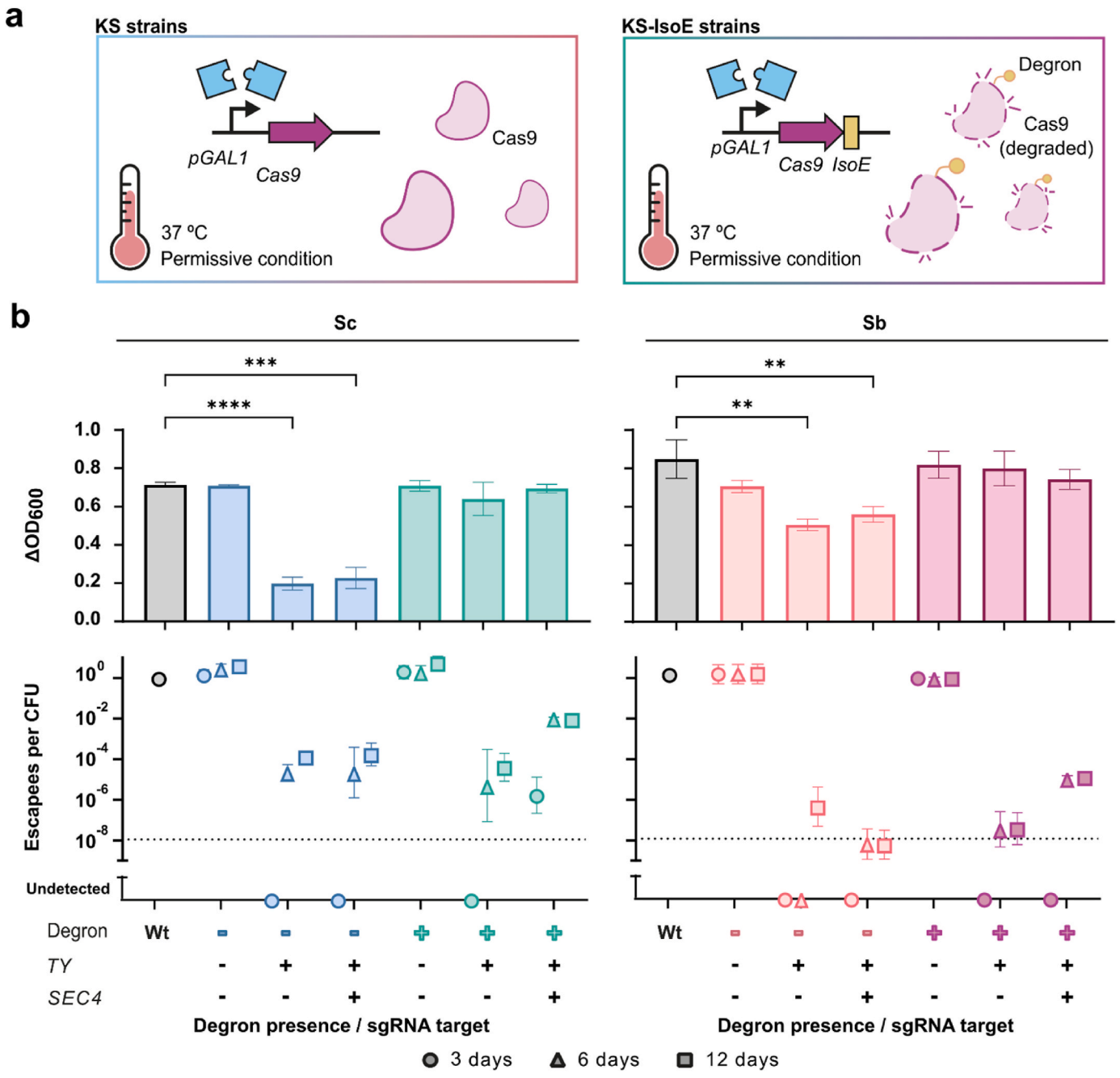

(caption on next page)

Fig. 3. The improved temperature-inducible CRISPR-Cas9 kill switch (KS-IsoE). Graphical representation of KS and KS-IsoE systems under permissive (uninduced) conditions**. Left** - In KS strains, the leaky activity of the *pGAL1* promoter results in background activity of Cas9. **Right** - In KS-IsoE strains, Cas9 produced by *pGAL1* leaky activity are degraded by the proteasome due to IsoE-tagging. **b** Difference in OD_{600} (ΔOD_{600}) and escape frequencies of both Sc and Sb containing the KS or KS-IsoE systems. **Top** - Differences between the final and initial OD_{600} were assessed under permissive conditions (37 °C) after 24 h of cultivation. An unpaired student's t-test was performed (**p ≤ 0.01, ***p ≤ 0.001, and ****p ≤ 0.0001, when no comparison line was traced results were non-significant). **Bottom** - Escape frequency determination under restrictive conditions (25 °C). Colonies were observed for up to twelve days. The assay limit was determined by the maximum CFUs plated, approximately 10^9. The black dotted line represents the NIH guideline for good containment. **c** Yeast dilution spot assay demonstrating the dependence on temperature of the KS-IsoE strains – incubation lasted 3 day **d** Doubling times of both Sc and Sb KS-IsoE strains cultivated under permissive conditions (37 °C) for 24 h. For all plots, values and error bars are the average and standard deviation of biological triplicates, respectively. ∅: no sgRNA. T: *TY*-targeting sgRNA. T + S: *TY* and *SEC4*-targeting sgRNAs.

escapees were undetected until day 6 of incubation, nevertheless, late escape on the order of 10^{-6} escapees/CFU could be observed after twelve days. The weaker performance of Sc TS-KS was not surprising, as Sc-based systems showcased higher escape rate frequencies in all circuits when compared to Sb. A reason for the disparity could be Sb's diploid genotype. Sb-based systems carry twice the amount of regulatory elements (i.e. Tet-On, Gal4M9, and Cas9-related genetic parts) present in Sc, which doesn't present this level of redundancy. This means fewer mutation events are necessary for Sc-based circuits to be bypassed. Ultimately, combining the TS and KS-IsoE systems into a two-input biocontainment system proved to be a highly effective strategy. Since both individual systems are based on different modes of action and constituting parts, an orthogonal and additive response of the TS-KS system was achieved.

Next, the system's fitness under permissive conditions was assessed. While achieving comparable cell densities (ΔOD_{600}) to the Wt after a culture period of 24 h, the doubling time of engineered cells was significantly higher than the Wt (Fig. 4d). Considering that each of the single biocontainment modules when evaluated separately did not lead to a significant impairment on the growth rate, we believe the observed phenotype is the result of the additive burden of both systems in the metabolism of the strains. Nevertheless, its impact on the long-term stability of the circuit was found to be negligible. When submitted to permissive conditions for up to twelve days (approximately 140 generations) before their plating on restrictive conditions, essentially no alteration in the frequency of escapees was observed (Fig. 4e, S11). This result indicates the growth impairment of TS-KS strains to be mild and ultimately not lead to selective pressures under permissive conditions. Given that the average industrial batch fermentation extends for four to five days, and that Sb's colonization in the GI tract is transient, lasting on average three to four days, the system should remain stable in most applications (Chisti, 2014; Durmusoglu et al., 2021a).

2.6. Biocontained strains express heterologous proteins in a robust manner

As a final step in the characterization of the biocontained strains, we investigated their efficiency in producing recombinant proteins. mRuby2 was used as a proxy for other proteins of interest. A strong constitutive promoter (*pTEF1*) was applied and both plasmid-based and genomic expression were evaluated. For plasmid-based expression, a high-copy (2micron) plasmid based on *LYS2* for lysine auxotrophy-based maintenance was used. For genomic integration, the intergenic region *INT1* described by Durmusoglu et al. was chosen as the integration *locus* due to its previous application in Sb and the availability of functional sgRNAs (Durmusoglu et al., 2021a). For both Sc and Sb, all safeguard circuits (TS, KS, and TS-KS) achieved mRuby2 expression levels equivalent to their Wt counterparts regardless of the expression system (Fig. 5a-b). This suggests that the biocontainment systems developed during this work exert no impact on protein production and can be employed in different applications.

3. Conclusions

Robust intrinsic biocontainment systems are determinant to the development of many biotechnological applications. Apart from their utility in traditional industrial processes (e.g. for the protection of intellectual property), their application in ascending fields that encompass the intentional environmental release of bioengineered microorganisms (e.g. eLPBs and bioremediation) is paramount (Lee et al., 2018; George et al., 2024). The TS, KS-IsoE, and TS-KS systems developed in this work add to the biocontainment toolbox already available for yeasts (Hedin et al., 2023b; Hoffmann and Cai, 2024; Chang et al., 2023; Agmon et al., 2017; Cai et al., 2015; Yoo et al., 2020). Nevertheless, unlike other designs, no auxotrophy based on molecules commonly found in the environment (e.g. sugars, vitamins, and AAs) or killing mechanisms dependent on artificial settings (e.g. the presence of a specific molecule) are employed. This unique feature makes the safeguard systems presented here particularly amenable to eLBPs.

To create orthogonal switches with redundant functionalities, we focused on two different modes of action: transcriptional control and DNA disruption. In a stepwise approach, single-input switches were separately developed, tested, and improved before their combination into a double-input switch. First, a transcription switch based on the control of the essential gene *RPC11* by an improved Tet-On system resulted in the restriction of cell survival to micromolar concentrations of aTc. Upon aTc removal, cells were effectively killed in approximately 16 h, leading to detectable escape frequencies only after six days of incubation. Next, a kill switch based on the control of Cas9-mediated death via a temperature-inducible *pGAL* promoter was constructed. The circuit takes advantage of the low repair efficiency of yeast's NEHJ machinery following DSBs caused by Cas9. The choice of genomic target of the provided sgRNAs was found to greatly interfere with the killing efficiency. The highest fatality rates were obtained when a sgRNA with multiple target sites was employed, suggesting that numerous concomitant DSBs cause intense burden in the repair machinery. In contrast, combining multiple sgRNAs with varied target sites reduced the system efficiency, most likely due to the low performance of multiplex CRISPR-Cas9 systems in yeast. After establishing the best sgRNA choice, the kill switch was further improved through the addition of a degron tag. This final step prevented the leaky activity of Cas9 under permissive conditions, ultimately improving the strains' fitness and long-term stability. Finally, both circuits were combined into a two-input switch. An additive effect was observed, and none or very few escapees were found - even after twelve days of incubation under restrictive conditions. Even though a slight fitness impairment was observed in TS-KS strains exposed to permissive conditions, the system was found to be stable for more than a hundred generations. For all systems, the production of heterologous proteins was achieved at levels comparable to the Wt, supporting their pertinence in varied applications.

All circuits were simultaneously engineered in two different yeast strains: laboratory Sc and probiotic Sb. The easiness of portability of the system suggests that industrial *S. cerevisiae* strains, regardless of ploidy, could be similarly engineered for this purpose. For all constructs, diploid Sb achieved escape frequencies significantly lower than haploid Sc, indicating that the redundancy of regulatory elements might play an important role in preventing the emergence of escape mutants. Various other biocontainment systems developed for different microorganisms support this finding (Foo et al., 2024; Rottinghaus et al., 2022; Agmon et al., 2017; Cai et al., 2015). In light of this discrepancy, one could

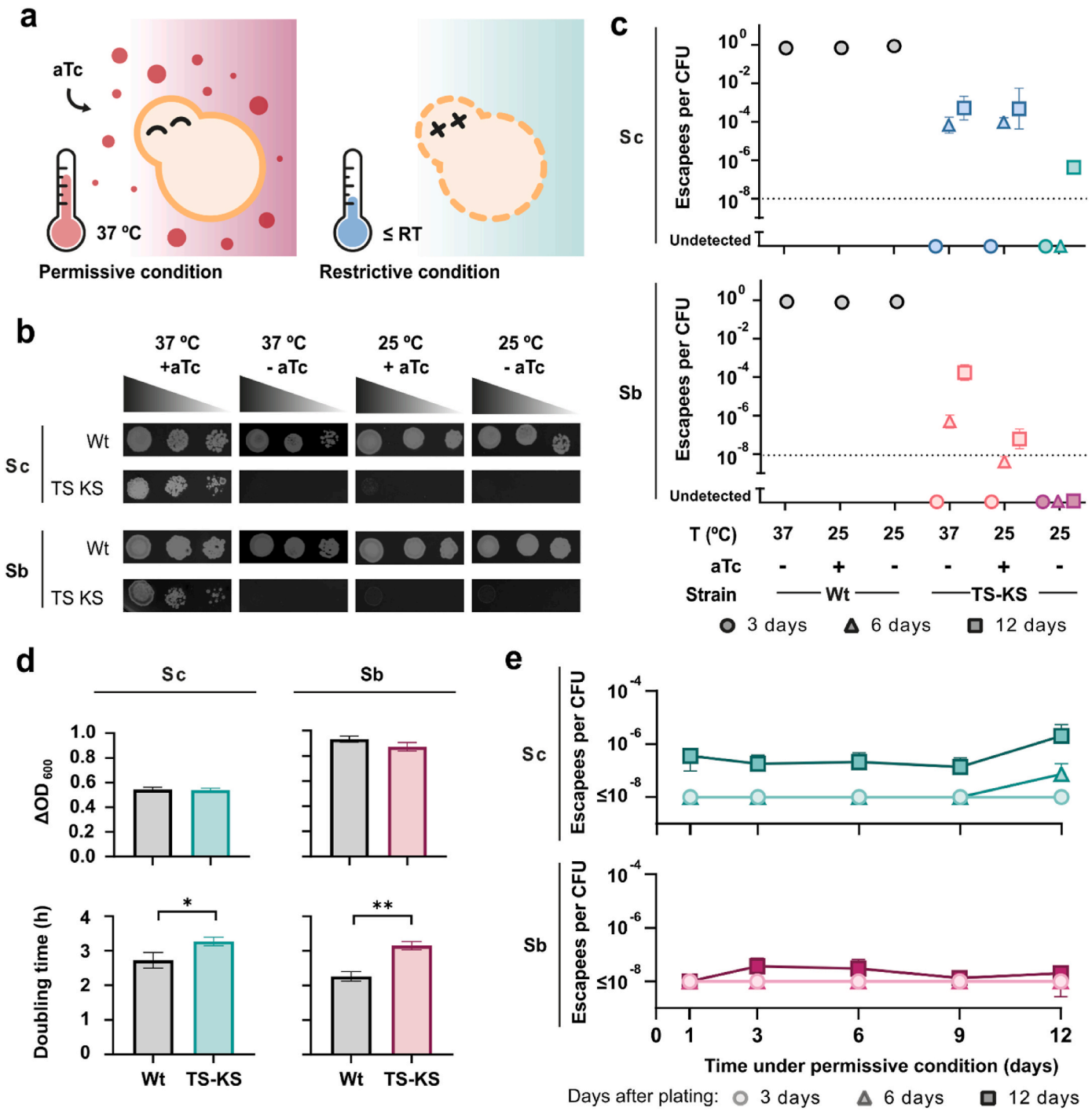

Fig. 4. The two-input aTc-restrained and temperature-induced biocontainment system (TS-KS). **a** A graphical scheme represents the functioning of the TS-KS system. When submitted to full permissive conditions (aTc, 37 °C) cells are able to survive. When transferred to partial (no aTc, 37 °C or aTc, 25 °C) or complete restrictive (no aTc, 25 °C) conditions, cells are no longer viable. **b** Dilution spot assay of Sc and Sb KS-IsoE strains. Plates were incubated for three days. **c** Escape frequencies of both Sc and Sb containing the TS-KS system. Colonies under partial or complete restrictive conditions were observed for up to twelve days. The assay limit was determined by the maximum CFUs plated, approximately 10^9. The black dotted line represents the NIH guideline for good containment. **d** Difference in OD_{600} (ΔOD_{600}) (**Top**) and doubling time (**bottom**) in hours of TS-KS strains assessed under permissive conditions after 24 h of cultivation. An unpaired student's t-test was performed (**$p \leq 0.01$, *$p \leq 0.05$, when no comparison line was traced results were non-significant). **e** Long-term stability assessment of TS-KS. Every three days for twelve days (approximately 144 generations) cells under fresh permissive conditions were plated on restrictive conditions. CFU quantification was performed three, six, and twelve days after plating. For all plots, values and error bars are the mean and standard deviation of biological triplicates, respectively.

envision the duplication of certain regulatory elements, such as the Cas9 or the Tet-regulator, as a mean to enhance the performance of Sc in future applications.

Another essential feature of robust safeguard systems lies in the effective biocontainment of recombinant nucleic acids to avoid horizontal gene transfer. All systems developed throughout this work cope with this directive by presenting regulatory parts integrated into the yeast genome. Only sgRNAs are delivered in plasmids, nevertheless, these depend on AA auxotrophy, and no antibiotic resistance cassette was employed. The specificity of the sgRNAs to Sc and Sb's genome and

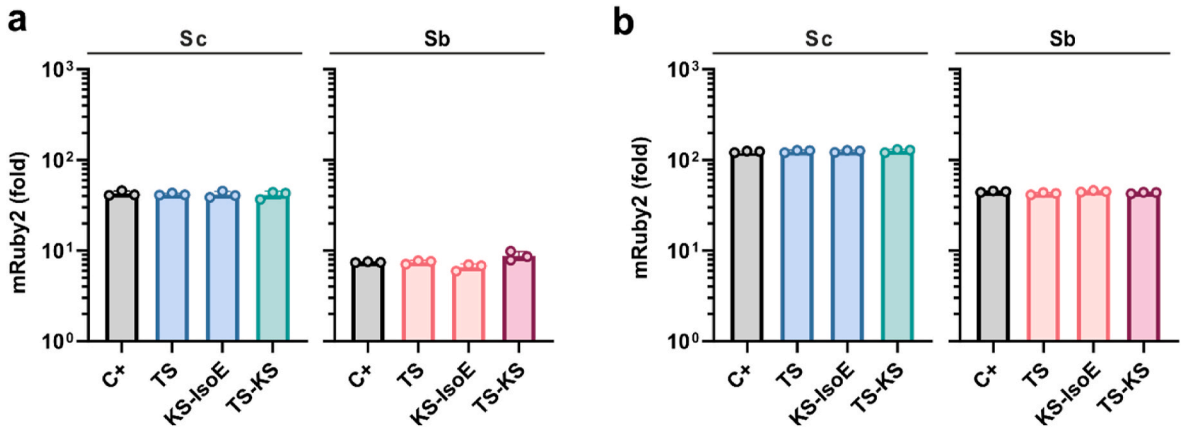

Fig. 5. Expression of a heterologous protein (mRuby2) by safeguard strains. Fold-change relative to a Wt strain. **a** *mRuby2* was integrated into the genome. **b** *mRuby2* was plasmid-expressed. For all plots, values and error bars are the mean and standard deviation of biological triplicates, respectively. C+: A Wt strain containing the *pTEF1-mRuby2* cassette integrated into the genome (**a**) or provided in a plasmid (**b**).

its functionality only in the presence of Cas9 also adds to its safety, as even in the rare case of transfer no effect should be expected in other organisms.

In summary, we developed robust biocontainment for Sc and Sb based on transcription and kill switches. The final two-input system allowed the selective elimination of the engineered yeast via either aTc removal or a drop in temperature while remaining stable at permissive conditions for more than a hundred generations. The modular aspect of the regulating parts (Tet-On and Gal4M9) supports their exchange for sensors targeting other chemical or environmental cues, ultimately allowing the killing or life-sustaining mechanisms developed in this work to be functional in other varied settings. On top of that, the use of a degron tag to overcome *pGal1* promoter background activity in uninduced conditions is, to our knowledge, an original application in yeast. We foresee that other inducible systems with similar leaky behavior might benefit from this strategy. When it comes to *in vivo* applications of therapeutic yeast, we believe the circuits developed in this work might be of great value to push forward safe transgenic probiotics. Previous publications on Sb-based eLBPs indicate that the *in vivo* performance of engineered Sb is comparable to *in vitro* conditions (Hedin et al., 2023a, 2023b; Chen et al., 2020b; Kim et al., 2023; Durmusoglu et al., 2021b). Nevertheless, the formulation and *in vivo* testing of the switches developed in this work remains an important future step for their transition from academic endeavor to industrial resource. Finally, the genomic analysis of escapees, including late escapees, also stands out as an important future direction to uncover the most common escape mechanisms and potentially improve the efficiency of the circuits developed in this work. Apart from that, the transcriptomic and proteomic assessment of the biocontained strains could substantiate our understanding of the underlying mechanisms behind the low efficiency of multiplex CRISPR-Cas9 systems or the functionality of the degron approach.

4. Methods

4.1. Strains, chemicals, and media

TOP10 *Escherichia coli* was used for all plasmid assemblies and maintenance. *E. coli* cells were grown in lysogeny broth (LB) at 37 °C. LB was supplemented with ampicillin (100 μg/mL) or kanamycin (50 μg/mL) when necessary – both from Carl Roth (Karlsruhe, Germany). Agar was added to 2 % for preparing solid media. All Sc strains are derived from BY4741 (MATa *leu2*Δ0 *met15*Δ0 *ura3*Δ0 *his3*Δ1) (Baker Brachmann et al., 1998). All Sb strains are derived from ATCC MYA796 (MATa/α) (McCullough et al., 1998). Yeast strains were cultured in yeast extract-peptone-dextrose (YPD) medium, or synthetic medium with dextrose (SD) supplemented with appropriate AAs – the latter was used in all characterization assays. Media were supplemented with 100 μg/mL nourseothricin (Jena Bioscience - Jena, Germany) when necessary. Agar was added to 2 % for preparing solid media. Yeast cultures were carried out at 30 °C for Sc or 37 °C for Sb unless stated otherwise (e.g. biocontainment evaluation assays were always carried out at 37 °C). aTc was purchased from Cayman chemical (Ann Arbor, MI, USA) and doxycycline (dox) from Sigma-Aldrich (Saint Louis, MO, USA).

4.2. Plasmids, repair fragments, and cloning in E. coli

All genetic parts relevant to this work are listed in Table S1. Plasmids are listed in Table S2. All gene strands and primers were purchased from Eurofins Genomics (Ebersberg, Germany). DNA amplification reactions were carried out with Q5 polymerase (New England Biolabs - Ipswich, MA, USA). Plasmid assembly was primarily carried out via AQUA cloning as described by Beyer et al., however, complicated constructs were cloned with the NEBuilder HiFi kit (New England Biolabs - Ipswich, MA, USA) (Beyer et al., 2015). *E. coli* cells were submitted to chemical transformation. Plasmid mini preparation from *E. coli* was performed with the Nucleospin Plasmid DNA Purification kit (Macherey-Nagel - Düren, Germany). Repair fragments for Cas9-mediated DSB repair were amplified from plasmids/genomic DNA with 55 bp homologies to the target *loci* as primer extensions. When KOs were performed, repair fragments were obtained in a templateless PCR reaction via the hybridization of primers containing 55 bp homologies to the target *loci*.

4.3. Construction of yeast strains

Yeast strains built in this work are listed in Table S3 and S4 sgRNAs used in this work are listed in Table S5. Genome edits via CRISPR-Cas9 were carried out via co-transformation of plasmid pRCC-N containing specific sgRNAs and repair fragments bearing 55 bp homologies to the target *loci* (Generoso et al., 2016). pRCC-N was a gift from Eckhard Boles (Addgene plasmid # 81192). CHOP-CHOP sgRNA designer (chopchop.cbu.uib.no) was used to design sgRNAs. Plasmids for the heterologous expression of sgRNAs and proteins were built over vector pXP418 (Fang et al., 2011). pXP418 was a gift from Nancy DaSilva & Suzanne Sandmeyer (Addgene plasmid # 26843). Sc transformation was carried out as described by Gietz et al. (Gietz and Schiestl, 2007). Sb transformation was carried out in a slightly modified protocol, in which all cultures were set to 37 °C, and the heat-shock period at 42 °C was increased by 20 min, similar to what described by Durmusoglu et al. (2021a). Whenever transformations were realized to obtain safeguard strains, transformed cells were kept on media containing permissive conditions for recovery and were also plated on permissive conditions. Sc genomic

DNA extractions for PCR-based applications were carried out via the protocol described by Lõoke et al. (2017), while Sb genomic DNA extractions followed the method communicated by Durmusoglu et al. (2021a).

4.4. Fluorescence measurements

The measurements of OD_{600} and fluorescence of mRuby2/yeGFP were performed on an Infinite MPlex microtiter plate reader (TECAN - Männedorf, Switzerland). Sterile, black 96-well plates with transparent flat-bottom were used, with 200 µl total culture volume. yeGFP readings were carried out with excitation at 488 nm and emission at 507 nm, while mRuby2 readings used excitation at 559 nm and emission at 600 nm. Fluorescence intensity was normalized to cell density. For the Tet-On system dose-response curves, cells were grown overnight (ON) in biological triplicates in SD-complete (SC), then diluted to $OD_{600} = 1$ in SC containing varying aTc/dox concentrations. After 6 h, cells were washed three times with phosphate-buffered saline (PBS), resuspended in PBS, and measurements were performed. For the characterization of the Gal4M9-based regulatory complex, cells were grown in biological triplicates ON in SC at 37 °C, then diluted to $OD_{600} = 1$ in SC pre-warmed to either 37, 26, or 24 °C and cultured in the respective temperatures. After 0, 6, 12, and 24 h, cells were washed three times with PBS, resuspended in PBS to $OD_{600} = 1$, and measurements were performed. For the evaluation of heterologous protein production of biocontained strains, cells were grown ON in biological triplicates in SD (ura^- for integrated reporter and ura^- lys^- for plasmid-expressed reporter) at 37 °C. The next day cells were washed three times with PBS, diluted to $OD_{600} = 1$ and measurements were performed.

4.5. Dilution spotting

Yeast cultures were grown in permissive condition in SC (for TS) or SD ura^- (for KS and TS-KS) at 37 °C ON, washed twice with PBS, and then diluted to $OD_{600} = 1$. These normalized cultures were used to make a 1:10 dilution series in sterile water. 5 µL of each dilution (the most concentrated spot presents approximately 5×10^4 CFUs, assuming a conversion factor of 10^7 CFU/mL/OD_{600}) were spotted on top of SC plates containing permissive and restrictive conditions. Plates were incubated for three days in appropriate conditions and subsequently imaged with the iBright FL1500 imaging system (Invitrogen - Waltham, MA, USA). For TS strains, a restrictive treatment was performed prior to plating. Briefly, cells were taken from permissive to restrictive liquid media for up to 24 h before plating on restrictive conditions. When the temperature-induced kill switch was evaluated, plates, liquid media, and water were pre-warmed to 37 °C. A heating pad was used to maintain plates warm while plating.

4.6. Quantification of RPC11 expression levels

Wt and TS strains were subjected in biological triplicates to a shift from permissive to restrictive conditions – 1 µg/mL aTc to no aTc. Approximately 10^8 CFUs were collected 0, 3, 6, 12, and 24 h after the switch. Samples were immediately frozen and stocked at −80 °C. Total RNA was recovered from each sample via a modified version of the protocol established by Wächtler et al. (2011). In resume, after thawing, cells were collected by centrifugation and washed once with RNA Lysis Buffer (RLA) (Promega – Madison, WI, USA). Cells were pelleted down and subsequentially resuspended in AE-buffer (50 mM Na-acetate pH 5.3, 10 mM EDTA, 1 % SDS). The suspension was added of phenol/-chloroform/isoamyl alcohol (25:24:1) and transferred to Phasemaker tubes (Thermo Fischer Scientific - Waltham, MA, USA). Tubes were heated at 65 °C for 5 min and immediately shock frozen for 10 min, this process was repeated 3 times. Next, cells were thawed at 65 °C and the aqueous phase was transferred to new tubes. RNA was precipitated by incubation in isopropanol and sodium acetate ON at −20 °C and washed twice with ethanol prior to elution in nuclease-free water. Afterward, a reverse transcription reaction for cDNA production was carried out alongside gDNA removal with the iScript gDNA clear cDNA synthesis kit (New England Biolabs - Ipswich, MA, USA). Finally, qPCR was carried out using the SsoAdvanced Universal SYBR Green Supermix (New England Biolabs - Ipswich, MA, USA) in a CFX96 Real-Time PCR Detection System (Bio-Rad - Hercules, CA, USA). The expression levels of the housekeeping gene *ALG9* were analyzed as a control (Teste et al., 2009). The mRNA level expression was calculated as fold-changes of cycle threshold (Ct) value relative to Wt by using the $2^{-\Delta\Delta CT}$ method (Livak and Schmittgen, 2001). Fold-change relative to permissive conditions was established by normalizing expression levels at different time points by time point 0 h.

4.7. Growth assessment

Growth curves across conditions were recorded in sterile transparent flat-bottom 96-well plates using 200 µl total culture volume in an Infinite MPlex microtiter plate reader (TECAN - Männedorf, Switzerland). Breathe-Easy air-penetrable seals (Diversified Biotech - Dedham, MA, USA) were used to seal the plates. Cells were seeded in biological triplicates at an $OD_{600} = 0.02$ and optical density at 600 nm was recorded every 30 min for 24 h. SC medium was employed for TS strains and SD ura^- for KS and TS-KS strains. All experiments were carried out at 37 °C with high orbital shaking (amplitude 3). When appropriate, aTc was added to 1 µg/mL. Blank medium was used as control. When the temperature-induced kill switch was evaluated, plates and media were pre-warmed to 37 °C. A heating pad was used to maintain plates warm while seeding.

4.8. Escape frequency determination

To determine the escape frequency of biocontained strains, cells were grown ON in biological triplicates at permissive conditions. SC medium was employed for TS strains and SD ura^- for KS and TS-KS strains. The next day, 100 CFUs of each replicate were plated onto permissive media - assuming a conversion factor of 10^7 CFU/mL/OD_{600}. Using the same conversion factor, 10^2 to 10^9 CFUs - in increments of two orders of magnitude - from each replicate were plated onto restrictive conditions. Following incubation of plates for three, six, or twelve days, CFUs were counted. The CFU values obtained for the control plates – permissive condition, were used to correct the conversion factor and to calculate the total number of cells plated. When the temperature-induced kill switch was evaluated, plates and media were pre-warmed to 37 °C. A heating pad was used to maintain control plates warm while plating.

4.9. Long-term stability assay

TS-KS strains were cultured in biological triplicates ON in 5 mL of permissive SD ura^- medium (37 °C, 1 µg/mL aTc). The next day cells were transferred to 20 mL of the same medium to an OD_{600} of 0.2. Every two days the transferring process was repeated. Every three days, 10^6-10^8 CFUs were plated on restrictive conditions (25 °C, no aTc) to assess for escapees - assuming a conversion factor of 10^7 CFU/mL/OD_{600}. The process was repeated for a total of twelve days – approximately 144 generations. After plating, cells were incubated at restrictive conditions for up to twelve days and CFUs were counted after three, six, and twelve days.

4.10. Statistical analysis

All statistical tests were performed using GraphPad Prism (La Jolla, CA, USA). All statistical details of experiments, including significance criteria and sample size can be found in the figure legends, methods section, or supplementary files.

CRediT authorship contribution statement

Carla Maneira: Writing – original draft, Visualization, Validation, Methodology, Investigation, Formal analysis, Conceptualization. **Sina Becker:** Investigation, Formal analysis. **Alexandre Chamas:** Writing – review & editing, Formal analysis. **Gerald Lackner:** Writing – review & editing, Supervision, Project administration, Funding acquisition, Conceptualization.

Data availability

All data supporting the findings of this study are available within the manuscript file and its supplementary information files. Source data are provided with this paper. Materials are available from the authors upon request.

Funding

Financial support to C.M. and G.L. was given by the German Federal Ministry of Education and Research within the funding program Photonics Research Germany, Project Leibniz Center for Photonics in Infection Research (Subproject LPI-BT5, contract number 13N15718). The LPI initiated by Leibniz-IPHT, Leibniz-HKI, UKJ, and FSU Jena is part of the BMBF national roadmap for research infrastructures. A.C. and G.L. also thank the Deutsche Forschungsgemeinschaft (DFG, German Research Foundation) under Germany's Excellence Strategy – EXC 2051 – Project-ID 390713860 for funding.

Declaration of competing interests

The authors declare no conflict of interests.

Acknowledgments

We would like to thank the NIH NIAID BIOART source collection for making available to the public domain the following illustrations used in this work: bioart.niaid.nih.gov/bioart/212 and bioart.niaid.nih.gov/bioart/79.

Appendix A. Supplementary data

Supplementary data to this article can be found online at https://doi.org/10.1016/j.ymben.2025.06.009.

Data availability

All data supporting the findings of this study are available within the manuscript file and its supplementary information files. Source data are provided with this paper.

References

Agmon, N., Tang, Z., Yang, K., Sutter, B., Ikushima, S., Cai, Y., Caravelli, K., Martin, J.A., Sun, X., Choi, W.J., et al., 2017. Low escape-rate genome safeguards with minimal molecular perturbation of *Saccharomyces cerevisiae*. Proc. Natl. Acad. Sci. U. S. A. 114. https://doi.org/10.1073/pnas.1621250114.

Baker Brachmann, C., Davies, A., Cost, G.J., Caputo, E., Li, J., Hieter, P., Boeke, J.D., 1998. Designer deletion strains derived from *Saccharomyces cerevisiae* S288C: a useful set of strains and plasmids for PCR-mediated gene disruption and other applications. Yeast 14, 115–132. https://doi.org/10.1002/(SICI)1097-0061(19980130)14:2<115::AID-YEA204>3.0.CO;2-2.

Baldera-Aguayo, P.A., Lee, A., Cornish, V.W., 2022. High-titer production of the fungal anhydrotetracycline, TAN-1612, in engineered yeasts. ACS Synth. Biol. 11, 2429–2444. https://doi.org/10.1021/acssynbio.2c00116.

Beyer, H.M., Gonschorek, P., Samodelov, S.L., Meier, M., Weber, W., Zurbriggen, M.D., 2015. AQUA cloning: a versatile and simple enzyme-free cloning approach. PLoS One 10, e0137652. https://doi.org/10.1371/journal.pone.0137652.

Cai, Y., Agmon, N., Choi, W.J., Ubide, A., Stracquadanio, G., Caravelli, K., Hao, H., Bader, J.S., Boeke, J.D., 2015. Intrinsic biocontainment: multiplex genome safeguards combine transcriptional and recombinational control of essential yeast genes. Proc. Natl. Acad. Sci. U. S. A. 112, 1803–1808. https://doi.org/10.1073/pnas.1424704112.

Chan, C.T.Y., Lee, J.W., Cameron, D.E., Bashor, C.J., Collins, J.J., 2016. 'Deadman' and 'Passcode' microbial kill switches for bacterial containment. Nat. Chem. Biol. 12, 82–86. https://doi.org/10.1038/nchembio.1979.

Chang, T., Ding, W., Yan, S., Wang, Y., Zhang, H., Zhang, Y., Ping, Z., Zhang, H., Huang, Y., Zhang, J., et al., 2023. A robust yeast biocontainment system with two-layered regulation switch dependent on unnatural amino acid. Nat. Commun. 14, 6487. https://doi.org/10.1038/s41467-023-42358-4.

Chen, K., Zhu, Y., Zhang, Y., Hamza, T., Yu, H., Saint Fleur, A., Galen, J., Yang, Z., Feng, H., 2020a. A probiotic yeast-based immunotherapy against *Clostridioides difficile* infection. Sci. Transl. Med. 12, eaax4905. https://doi.org/10.1126/scitranslmed.aax4905.

Chen, K., Zhu, Y., Zhang, Y., Hamza, T., Yu, H., Fleur, A. Saint, Galen, J., Yang, Z., Feng, H., 2020b. A probiotic yeast-based immunotherapy against Clostridioides difficile infection. Sci. Transl. Med. 12. https://doi.org/10.1126/scitranslmed.aax4905. http://www.ncbi.nlm.nih.gov/pubmed/33115949.

Chisti, Y., 2014. Fermentation (industrial) | basic considerations. In: Encyclopedia of Food Microbiology. Elsevier, pp. 751–761. https://doi.org/10.1016/B978-0-12-384730-0.00106-3.

Chopra, I., 1994. Tetracycline analogs whose primary target is not the bacterial ribosome. Antimicrob. Agents Chemother. 38, 637–640. https://doi.org/10.1128/AAC.38.4.637.

Christiano, R., Nagaraj, N., Fröhlich, F., Walther, T.C., 2014. Global proteome turnover analyses of the yeasts *S. cerevisiae* and *S. pombe*. Cell Rep. 9, 1959–1965. https://doi.org/10.1016/j.celrep.2014.10.065.

Clarke, L., Kitney, R., 2020. Developing synthetic biology for industrial biotechnology applications. Biochem. Soc. Trans. 48, 113–122. https://doi.org/10.1042/BST20190349.

Dicarlo, J.E., Norville, J.E., Mali, P., Rios, X., Aach, J., Church, G.M., 2013. Genome engineering in *Saccharomyces cerevisiae* using CRISPR-cas systems. Nucleic Acids Res. 41, 4336–4343. https://doi.org/10.1093/nar/gkt135.

Dinh, Q., Moreau-Guigon, E., Labadie, P., Alliot, F., Teil, M.-J., Blanchard, M., Eurin, J., Chevreuil, M., 2017. Fate of antibiotics from hospital and domestic sources in a sewage network. Sci. Total Environ. 575, 758–766. https://doi.org/10.1016/j.scitotenv.2016.09.118.

Durmusoglu, D., Al'Abri, I.S., Collins, S.P., Cheng, J., Eroglu, A., Beisel, C.L., Crook, N., 2021a. *In situ* biomanufacturing of small molecules in the mammalian gut by probiotic *saccharomyces boulardii*. ACS Synth. Biol. 10, 1039–1052. https://doi.org/10.1021/acssynbio.0c00562.

Durmusoglu, D., Al'Abri, I.S., Collins, S.P., Cheng, J., Eroglu, A., Beisel, C.L., Crook, N., 2021b. In situ biomanufacturing of small molecules in the mammalian gut by probiotic saccharomyces boulardii. ACS Synth. Biol. 10, 1039–1052. https://doi.org/10.1021/acssynbio.0c00562.

Fang, F., Salmon, K., Shen, M.W.Y., Aeling, K.A., Ito, E., Irwin, B., Tran, U.P.C., Hatfield, G.W., Da Silva, N.A., Sandmeyer, S., 2011. A vector set for systematic metabolic engineering in *Saccharomyces cerevisiae*. Yeast 28, 123–136. https://doi.org/10.1002/yea.1824.

Foo, G.W., Leichthammer, C.D., Saita, I.M., Lukas, N.D., Batko, I.Z., Heinrichs, D.E., Edgell, D.R., 2024. Intein-based thermoregulated meganucleases for containment of genetic material. Nucleic Acids Res. 52, 2066–2077. https://doi.org/10.1093/nar/gkad1247.

Gallagher, R.R., Patel, J.R., Interiano, A.L., Rovner, A.J., Isaacs, F.J., 2015. Multilayered genetic safeguards limit growth of microorganisms to defined environments. Nucleic Acids Res. 43, 1945–1954. https://doi.org/10.1093/nar/gku1378.

Generoso, W.C., Gottardi, M., Oreb, M., Boles, E., 2016. Simplified CRISPR-cas genome editing for *Saccharomyces cerevisiae*. J. Microbiol. Methods 127, 203–205. https://doi.org/10.1016/j.mimet.2016.06.020.

George, D.R., Danciu, M., Davenport, P.W., Lakin, M.R., Chappell, J., Frow, E.K., 2024. A bumpy road ahead for genetic biocontainment. Nat. Commun. 15. https://doi.org/10.1038/s41467-023-44531-1.

Gietz, R.D., Schiestl, R.H., 2007. High-efficiency yeast transformation using the LiAc/SS carrier DNA/PEG method. Nat. Protoc. 2, 31–34. https://doi.org/10.1038/nprot.2007.13.

Gossen, M., Bujard, H., 1993. Anhydrotetracycline, a novel effector for tetracycline controlled gene expression systems in eukaryotic cells. Nucleic Acids Res. 21, 4411–4412. https://doi.org/10.1093/nar/21.18.4411.

Hedin, K.A., Zhang, H., Kruse, V., Rees, V.E., Bäckhed, F., Greiner, T.U., Vazquez-Uribe, R., Sommer, M.O.A., 2023a. Cold exposure and oral delivery of GLP-1R agonists by an engineered probiotic yeast strain have antiobesity effects in mice. ACS Synth. Biol. 12, 3433–3442. https://doi.org/10.1021/acssynbio.3c00455.

Hedin, K.A., Kruse, V., Vazquez-Uribe, R., Sommer, M.O.A., 2023b. Biocontainment strategies for *in vivo* applications of *Saccharomyces boulardii*. Front. Bioeng. Biotechnol. 11, 1136095. https://doi.org/10.3389/fbioe.2023.1136095.

Hoffmann, S.A., Cai, Y., 2024. Engineering stringent genetic biocontainment of yeast with a protein stability switch. Nat. Commun. 15, 1060. https://doi.org/10.1038/s41467-024-44988-8.

Hudson, L.E., McDermott, C.D., Stewart, T.P., Hudson, W.H., Rios, D., Fasken, M.B., Corbett, A.H., Lamb, T.J., 2016. Characterization of the probiotic yeast *Saccharomyces boulardii* in the healthy mucosal immune system. PLoS One 11. https://doi.org/10.1371/journal.pone.0153351.

Hwang, I.Y., Koh, E., Wong, A., March, J.C., Bentley, W.E., Lee, Y.S., Chang, M.W., 2017. Engineered probiotic *Escherichia coli* can eliminate and prevent *Pseudomonas aeruginosa* gut infection in animal models. Nat. Commun. 8, 15028. https://doi.org/10.1038/ncomms15028.

Isabella, V.M., Ha, B.N., Castillo, M.J., Lubkowicz, D.J., Rowe, S.E., Millet, Y.A., Anderson, C.L., Li, N., Fisher, A.B., West, K.A., et al., 2018. Development of a synthetic live bacterial therapeutic for the human metabolic disease phenylketonuria. Nat. Biotechnol. 36, 857–867. https://doi.org/10.1038/nbt.4222.

Katz, L., Chen, Y.Y., Gonzalez, R., Peterson, T.C., Zhao, H., Baltz, R.H., 2018. Synthetic biology advances and applications in the biotechnology industry: a perspective. J. Ind. Microbiol. Biotechnol. 45, 449–461. https://doi.org/10.1007/s10295-018-2056-y.

Kim, J., Atkinson, C., Miller, M.J., Kim, K.H., Jin, Y.-S., 2023. Microbiome engineering using probiotic yeast: *saccharomyces boulardii* and the secreted human lysozyme lead to changes in the gut microbiome and metabolome of mice. Microbiol. Spectr. 11, e00780. https://doi.org/10.1128/spectrum.00780-23, 23.

Lee, J.W., Chan, C.T.Y., Slomovic, S., Collins, J.J., 2018. Next-generation biocontainment systems for engineered organisms. Nat. Chem. Biol. 14, 530–537. https://doi.org/10.1038/s41589-018-0056-x.

Lemos, B.R., Kaplan, A.C., Bae, J.E., Ferrazzoli, A.E., Kuo, J., Anand, R.P., Waterman, D. P., Haber, J.E., 2018. CRISPR/Cas9 cleavages in budding yeast reveal templated insertions and strand-specific insertion/deletion profiles. Proc. Natl. Acad. Sci. U. S. A. 115, E2010–E2047. https://doi.org/10.1073/pnas.1716855115.

Lim, B., Zimmermann, M., Barry, N.A., Goodman, A.L., 2017. Engineered regulatory systems modulate gene expression of human commensals in the gut. Cell 169, 547–558.e15. https://doi.org/10.1016/j.cell.2017.03.045.

Livak, K.J., Schmittgen, T.D., 2001. Analysis of relative gene expression data using real-time quantitative PCR and the 2-ΔΔCT method. Methods 25, 402–408. https://doi.org/10.1006/meth.2001.1262.

Lõoke, M., Kristjuhan, K., Kristjuhan, A., 2017. Extraction of genomic DNA from yeasts for PCR-based applications. Biotechniques 62. https://doi.org/10.2144/000114497.

Malyshev, D.A., Dhami, K., Lavergne, T., Chen, T., Dai, N., Foster, J.M., Corrêa, I.R., Romesberg, F.E., 2014. A semi-synthetic organism with an expanded genetic alphabet. Nature 509, 385–388. https://doi.org/10.1038/nature13314.

Mandell, D.J., Lajoie, M.J., Mee, M.T., Takeuchi, R., Kuznetsov, G., Norville, J.E., Gregg, C.J., Stoddard, B.L., Church, G.M., 2015. Biocontainment of genetically modified organisms by synthetic protein design. Nature 518, 55–60. https://doi.org/10.1038/nature14121.

Maneira, C., Chamas, A., Lackner, G., 2025. Engineering *Saccharomyces cerevisiae* for medical applications. Microb. Cell Fact. 24, 12. https://doi.org/10.1186/s12934-024-02625-5.

Mans, R., Van Rossum, H.M., Wijsman, M., Backx, A., Kuijpers, N.G.A., Van Den Broek, M., Daran-Lapujade, P., Pronk, J.T., Van Maris, A.J.A., Daran, J.-M.G., 2015. CRISPR/Cas9: a molecular Swiss army knife for simultaneous introduction of multiple genetic modifications in *Saccharomyces cerevisiae*. FEMS Yeast Res. 15. https://doi.org/10.1093/femsyr/fov004.

McCullough, M.J., Clemons, K.V., McCusker, J.H., Stevens, D.A., 1998. Species identification and virulence attributes of *Saccharomyces boulardii* (nom. inval.). J. Clin. Microbiol. 36, 2613–2617. https://doi.org/10.1128/JCM.36.9.2613-2617.1998.

Meddows, T.R., Savory, A.P., Lloyd, R.G., 2004. RecG helicase promotes DNA double-strand break repair. Mol. Microbiol. 52, 119–132. https://doi.org/10.1111/j.1365-2958.2003.03970.x.

Mnaimneh, S., Davierwala, A.P., Haynes, J., Moffat, J., Peng, W.-T., Zhang, W., Yang, X., Pootoolal, J., Chua, G., Lopez, A., et al., 2004. Exploration of essential gene functions via titratable promoter alleles. Cell 118, 31–44. https://doi.org/10.1016/j.cell.2004.06.013.

Peter, S.A., Isaac, J.S., Narberhaus, F., Weigand, J.E., 2021. A novel, universally active C-terminal protein degradation signal generated by alternative splicing. J. Mol. Biol. 433. https://doi.org/10.1016/j.jmb.2021.166890.

Rebeck, O.N., Wallace, M.J., Prusa, J., Ning, J., Evbuomwan, E.M., Rengarajan, S., Habimana-Griffin, L., Kwak, S., Zahrah, D., Tung, J., et al., 2024. A yeast-based oral therapeutic delivers immune checkpoint inhibitors to reduce intestinal tumor burden. Cell Chem. Biol.

Riglar, D.T., Giessen, T.W., Baym, M., Kerns, S.J., Niederhuber, M.J., Bronson, R.T., Kotula, J.W., Gerber, G.K., Way, J.C., Silver, P.A., 2017. Engineered bacteria can function in the mammalian gut long-term as live diagnostics of inflammation. Nat. Biotechnol. 35, 653–658. https://doi.org/10.1038/nbt.3879.

Roney, I.J., Rudner, A.D., Couture, J.F., Kærn, M., 2016. Improvement of the reverse tetracycline transactivator by single amino acid substitutions that reduce leaky target gene expression to undetectable levels. Sci. Rep. 6. https://doi.org/10.1038/srep27697.

Rottinghaus, A.G., Ferreiro, A., Fishbein, S.R.S., Dantas, G., Moon, T.S., 2022. Genetically stable CRISPR-based kill switches for engineered microbes. Nat. Commun. 13. https://doi.org/10.1038/s41467-022-28163-5.

Rovner, A.J., Haimovich, A.D., Katz, S.R., Li, Z., Grome, M.W., Gassaway, B.M., Amiram, M., Patel, J.R., Gallagher, R.R., Rinehart, J., et al., 2015. Recoded organisms engineered to depend on synthetic amino acids. Nature 518, 89–93. https://doi.org/10.1038/nature14095.

Ryan, O.W., Skerker, J.M., Maurer, M.J., Li, X., Tsai, J.C., Poddar, S., Lee, M.E., DeLoache, W., Dueber, J.E., Arkin, A.P., et al., 2014. Selection of chromosomal DNA libraries using a multiplex CRISPR system. eLife 3, e03703. https://doi.org/10.7554/eLife.03703.

Savage, T.M., Vincent, R.L., Rae, S.S., Huang, L.H., Ahn, A., Pu, K., Li, F., De Los Santos-Alexis, K., Coker, C., Danino, T., et al., 2023. Chemokines expressed by engineered bacteria recruit and orchestrate antitumor immunity. Sci. Adv. 9, eadc9436. https://doi.org/10.1126/sciadv.adc9436.

Scott, B.M., Gutiérrez-Vázquez, C., Sanmarco, L.M., Da Silva Pereira, J.A., Li, Z., Plasencia, A., Hewson, P., Cox, L.M., O'Brien, M., Chen, S.K., et al., 2021. Self-tunable engineered yeast probiotics for the treatment of inflammatory bowel disease. Nat. Med. 27, 1212–1222. https://doi.org/10.1038/s41591-021-01390-x.

Stirling, F., Bitzan, L., O'Keefe, S., Redfield, E., Oliver, J.W.K., Way, J., Silver, P.A., 2017. Rational design of evolutionarily stable microbial kill switches. Mol. Cell 68, 686–697.e3. https://doi.org/10.1016/j.molcel.2017.10.033.

Teste, M.A., Duquenne, M., François, J.M., Parrou, J.L., 2009. Validation of reference genes for quantitative expression analysis by real-time RT-PCR in *Saccharomyces cerevisiae*. BMC Mol. Biol. 10, 99. https://doi.org/10.1186/1471-2199-10-99.

Tscherner, M., Giessen, T.W., Markey, L., Kumamoto, C.A., Silver, P.A., 2019. A synthetic system that senses *Candida albicans* and inhibits virulence factors. ACS Synth. Biol. 8, 434–444. https://doi.org/10.1021/acssynbio.8b00457.

Wächtler, B., Wilson, D., Haedicke, K., Dalle, F., Hube, B., 2011. From attachment to damage: defined genes of *Candida albicans* mediate adhesion, invasion and damage during interaction with oral epithelial cells. PLoS One 6. https://doi.org/10.1371/journal.pone.0017046.

Wilson, D.J., 1993. NIH Guidelines for Research Involving Recombinant DNA Molecules, 2–3.

Xu, J., Xu, Y., Wang, H., Guo, C., Qiu, H., He, Y., Zhang, Y., Li, X., Meng, W., 2015. Occurrence of antibiotics and antibiotic resistance genes in a sewage treatment plant and its effluent-receiving river. Chemosphere 119, 1379–1385. https://doi.org/10.1016/j.chemosphere.2014.02.040.

Yoo, J.I., Seppälä, S., O'Malley, M.A., 2020. Engineered fluoride sensitivity enables biocontainment and selection of genetically-modified yeasts. Nat. Commun. 11, 5459. https://doi.org/10.1038/s41467-020-19271-1.

Zhou, P., Xie, W., Yao, Z., Zhu, Y., Ye, L., Yu, H., 2018. Development of a temperature-responsive yeast cell factory using engineered Gal4 as a protein switch. Biotechnol. Bioeng. 115, 1321–1330. https://doi.org/10.1002/bit.26544.